Applied Numerical Mathematics 133 (2018) 41–51

Contents lists available at ScienceDirect

Applied Numerical Mathematics

www.elsevier.com/locate/apnum

Mathematical modeling and numerical simulation of the TGF-β/Smad signaling pathway in tumor microenvironments

Adnan Morshed [a], Prashanta Dutta [a], Robert H. Dillon [b,*]

[a] School of Mechanical and Materials Engineering, Washington State University, Pullman, WA 99164-2920, United States
[b] Department of Mathematics and Statistics, Washington State University, Pullman, WA 99164-2920, United States

ARTICLE INFO

Article history:
Available online 20 November 2017

Keywords:
Immersed interface method
TGF-β
Smad
TGF-β/Smad
Tumor
Mathematical modeling
Tumor microenvironment

ABSTRACT

Mammalian cells respond in a variety of ways to concentrations of activated transforming growth factor (TGF) in the extracellular domain via intracellular Smad signaling pathways. TGF-β/Smad interaction is prevalent in a wide range of tumor environments with both autocrine and paracrine mechanisms driving temporal evolution. TGF-β has been reported to exhibit both pro- and antagonistic roles in tumor progression and survival. It has been argued that tumor cells upregulate TGF-β production by modifying the TGF-β/Smad pathway. Although several numerical studies of the tumor microenvironment have been conducted, most are based on PDEs where the cells are represented as a continuum or on discrete agent-based methods. Here, we develop a hybrid/cells-based model for the tumor microenvironment with cells represented as discrete entities in which diffusion and reaction in the extracellular environment as well as protein/receptor surface interactions are described using immersed interface methods. We develop a model for the cellular TGF-β/Smad pathways with the intracellular processes represented by systems of ODE's. In this study, we investigate the variation in cellular response with different levels of TGF-β in the extracellular environment. Our numerical results show that the model can account for experimental results on tumor cell lines when intracellular production and secretion of TGF-B based on activated Smad concentrations are included in the model system. Additionally, we studied the intracellular and surface levels of TGF-β in two different types of cells and observed variation in the extracellular domain.

1. Introduction

The cellular microenvironment is a versatile and responsive system that continuously senses its biochemical and mechanical state, transduces the extracellular signals into intracellular signals, and integrates these signals. The intracellular response to these signals may involve changes in metabolic state, gene expression, growth, differentiation, cell division, cell movement, and programmed cell death [19]. Cellular mutations as well as viral and bacterial agents can disrupt these processes and initiate the process of cancer. Most cells in the body are susceptible to mutations. Thus, different types of cancer have different features and unique cell types. Development of cancer in many tissues is highly dependent on the surrounding microenvironment as well [3,2]. In breast cancer, the transforming growth factor TGF-B plays a critical role in the transition from ductal carcinoma in situ (DCIS) to invasive ductal carcinoma (IDC). Stromal fibroblasts surrounding the

* Corresponding author.
E-mail addresses: adnan.morshed@wsu.edu (A. Morshed), Prashanta@wsu.edu (P. Dutta), dillon@math.wsu.edu (R.H. Dillon).

https://doi.org/10.1016/j.apnum.2017.11.004
0168-9274/

ducts convert to carcinoma-associated fibroblasts (CAFs) which in turn remodel the local microenvironment and facilitate the transition to IDC [20]. The transformation growth factor (TGF) is an important factor in many cancers that controls a diverse set of cellular processes including cell proliferation, recognition, differentiation, apoptosis, and specification of developmental fate [32,28].

Transforming growth factor is a member of the cytokine family whose members are key players in epithelial and neural tissues, the immune system and wound repair [25]. More than 30 different factors make up the human TGF-β superfamily [35]. Virtually all human cell types are responsive to TGF-β since it maintains tissue homeostasis and prevents benign tumors from progressing to malignancy by regulating cellular proliferation, differentiation, survival, and the overall microenvironment. But cancer cells suppress the influence of the TGF-β pathway by inactivating some core components, or by disabling the pathway's tumor-suppressive function. With TGF-β's antitumorigenic function suppressed, cancer cells can use the remaining TGF-β functionalities to their advantage in invasion, producing autocrine mitogens, or releasing prometastatic cytokines [23]. Cells that produce high levels of TGF-β may be shielded from the immune response [25]. Moreover, pathological forms of TGF-β signaling in immune cells promote chronic inflammation and the production of a protumorigenic environment. Tumor-derived TGF-β attract other stromal cell types such as myofibroblasts (at the invading tumor front) and osteoclasts (in bone metastases), resulting in much more effective spread. Thus, the TGF-β pathway has both anti- and protumoral activities [14,29]. In early-stage tumors, the TGF-β pathway promotes cell cycle arrest and apoptosis. In contrast, by promoting cancer cell motility, invasion, and epithelial-to-mesenchymal transition (EMT), the TGF-β pathway promotes tumor progression and metastasis in the later stages [33,10,16].

Several experimental studies have explored TGF interactions with its primary intracellular mediator proteins known as Smad [32,6]. Cellular Smads include the receptor-regulated R-Smads (Smad2, Smad3), the common mediator Smads (Co-Smad, Smad4) and inhibitor Smads (I-Smad, Smad7) [11]. Without TGF stimulation, the Smads are primarily located in the cytoplasm [27]. However, upon binding of TGF-β with cell surface receptors (TGF-β receptor I and TGF-β receptor II), the TGF-β-receptor complex phosphorylates Smad2 and Smad3. Phosphorylation facilitates Smad4 binding and accumulation in the nucleus. Nuclear Smad complexes regulate the transcription of TGF target genes. At the same time Smad complexes are dissociated and dephosphorylated by a nuclear phosphatase [15]. Experimental results indicate that cellular response to TGF-β depends both on the ligand concentration [7], as well as the duration of exposure [38]. However, there are still a number of important questions that remain unanswered. For instance, it is still unclear how specific genetic modifications in cancer cells alter the TGF-β signaling pathways. To this end, a number of mathematical models have been proposed to study and explain cellular behavior in TGF-β signaling [5,34]. Earlier models did not explicitly include TGF ligand dynamics account [38]. The model proposed by Schmierer et al. included nuclear-cytoplasmic Smad shuttling and compared numerical data with experimental results [30]. Zi et al. extended this model by incorporating TGF-β depletion and modification for alternating ligand exposure [38]. More recently, Kim and Othmer [18] combined the TGF-β/Smad pathway with epidermal growth factor (EGF) interactions for ductal carcinoma in situ (DCIS). Unlike the previous intracellular models, Kim and Othmer incorporated cross-talk between stromal and tumor cells, an important feature of in vivo tumor growth. The cells were represented as point sources but the model neglected TGF-β production and autocrine signaling.

In the present work, we investigate the spatio-temporal behavior of the cellular microenvironment with an active TGF-β/Smad pathway using a hybrid mathematical model. The cells are represented as discrete entities with finite size. Receptor internalization and recycling is included in the model as well as TGF-β degradation in the extracellular domain. The intracellular reaction network was coupled with the extracellular domain through reactions at the cell membrane. The model is validated using experimental results for several levels of TGF-β. Modeling cells as discrete dimensional bodies in the domain as opposed to point sources facilitates the investigation of the spatial interaction between cells in a more realistic way. For example, the effect of intercellular distance on cellular mutation observed experimentally [31] can be investigated using this approach. In addition, the use of finite dimensional cells will enable the extension of the model to study contiguous blocks of cells as seen in tumor cultures and in vivo tumor sections.

The rest of the paper is arranged as follows. In Section 2, we present the mathematical formulation for the model which includes TGF-β transport in the extracellular matrix (ECM), TGF-β ligand binding with membrane bound receptors, phosphorylation of Smad in the intracellular domain as well as production and secretion of TGF-β. In Section 3, we introduce a hybrid numerical method for solving the model system using an immersed interface method to solve the PDE's in the extracellular domain with ODE systems for the reaction kinetics on the cell surface and intracellular domain. In Section 4, we compare experimental data with numerical results and explore interactions of two cell types to explore the possibility of tumor mediated change to stromal cells in the proliferative and metastatic stages of tumor development.

2. Mathematical model

The domain considered in our model is a rectangular region with periodic boundaries as shown in Fig. 1. One or more cells with circular membrane are placed within the domain. In the extracellular matrix (ECM), TGF-β diffuses and reacts with cell surface receptors. The specific reactions include the binding of TGF ligands to receptors, the dissociation of the TGF-receptor complex and secretion of intracellular TGF-β into the extracellular domain. These reactions are captured as singular source terms along the cell surface in the reaction-diffusion equation for TGF-β using a two-dimensional delta

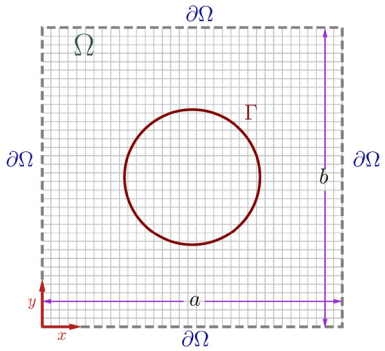

Fig. 1. Rectangular periodic computational domain Ω used to model the cellular microenvironment. The cells in the domain have a finite size where the cellular boundaries denoted by Γ. The cell diameter is 10 μm while the domain dimensions $a = b = 100$ μm. Cell membrane location in the regular Cartesian domain was calculated using spline interpolation [22].

Table 1
Species considered in the model and their symbols.

Notation	Description	Initial concentration (nM)
$TGF\ \beta, T$	Transforming Growth Factor β	0.01–0.2 [6]
R	Cell Surface TGF Receptor	0.2 [39]
TR	TGF-Receptor Complex	0.01
TRS	TGF-Receptor-SMAD complex	0.0
$Smad, S$	Intracellular Smad	492 [39]
$pSmad, S_P$	Phosphorylated Smad	0.0
T^{in}	Intracellular TGF	0.0

Table 2
Parameters required for the calculation of intracellular reaction and extracellular transport.

Parameter	Value	Reference
k_1^+	3.0×10^{-2} nM^{-1} min^{-1}	[8]
k_1^-	2.4×10^{-1} min^{-1}	[18]
k_T^+	2.4×10^{-2} nM^{-1} min^{-1}	[18]
k_T^-	3.96×10^{-1} min^{-1}	[18]
k_T^0	2.4×10^{-1} min^{-1}	[18]
k_S	3.96×10^{-1}–3.96×10^{1} min^{-1}	[18]
k_d	0.5 min^{-1}	Estimated
k_3	1.0 min^{-1}	Estimated
γ_1	4.0×10^{-3} min^{-1}	Estimated
r_1	1.0×10^{-3}	Estimated
r_2	5.0×10^{-3} nM	Estimated
n	7.0	Estimated
D_T	1.28×10^{-9} m^2/min	[1]

function. Moreover, the model provides for degradation of TGF-β in the ECM as a sink term in the extracellular domain. The general governing equation for the transport of TGF-β can be written as,

$$\nabla \cdot \left[-D_T \nabla T(\bar{x}, t)\right] = \int_\Gamma \left(k_1^- T R - k_1^+ T \cdot R + k_3 T^{in}\right)\delta\{x - x(s)\}\delta\{y - y(s)\}ds - \gamma_1 T(\bar{x}, t) \tag{2.1}$$

Here $T(\bar{x}, t)$ and T^{in} are the extracellular and spatially uniform intracellular TGF-β concentrations respectively and R is the unbound receptor concentration. The terms in the right-hand side inside the integral represent reversible TGF-β binding reactions on the cell surface and the secretion of intracellular TGF-β. $x(s)$ and $y(s)$ are the Lagrangian parameterizations of the cell boundary Γ. The second term is the extracellular TGF-β degradation with a rate γ_1. D_T is TGF-β diffusivity which is assumed constant over the domain. Full names of all symbols are listed in Table 1 and the numerical values of all the parameters are included in Table 2.

The interface conditions along the cell membrane for TGF-β include the jump in concentration, and jump in the normal flux across the membrane.

$$[T] = T^{out} - T^{in} = w(s) \tag{2.2}$$

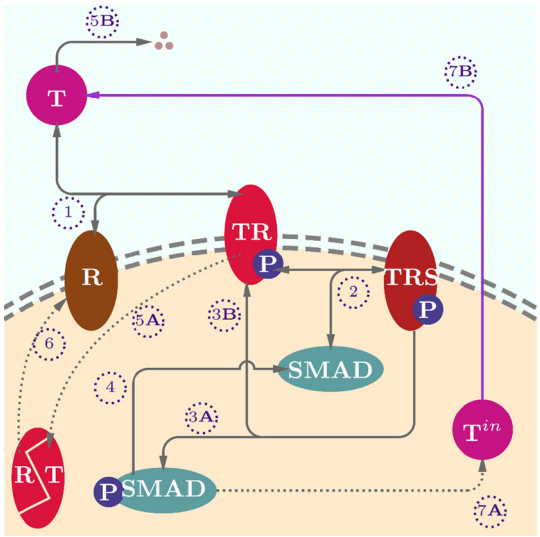

Fig. 2. Schematic of the basic TGF reaction pathways. (1) Extracellular TGF-β (T) reversibly binds with receptors (R) on the cell surface to produce TGF-β-receptor complex (TR); (2) The activated TR complex signals for Smad phosphorylation through reversibly forming a TR-Smad intermediate species (TRS); (3A, 3B) Phosphorylation of Smad, and (4) Dephosphorylation of Smad through phosphatase; (5A) TGF-receptor complex endocytosis is followed by its breakdown and degradation; (5B) Degradation of extracellular TGF-β; (6) Receptors are recycled to the surface; (7A) Phosphorylated Smad mediated transcriptional activities leads to intracellular TGF production which is eventually secreted (7B) to the extracellular environment.

$$\left[D\frac{\partial T}{\partial n}\right] = D_{T,out}\frac{\partial T^{out}}{\partial n} - D_{T,in}\frac{\partial T^{in}}{\partial n} = v(s) \tag{2.3}$$

Here $w(s)$ and $v(s)$ are functions defined across the interface. As described in Section 3, $w(s)$ is calculated from the changes in TGF-β concentration across the membrane and $v(s)$ from the membrane source terms in Eq. (2.1).

The intracellular biochemistry is complex and it depends on both internal and external environments. Active TGF-β dimer initiates the signaling cascade by bringing together two pairs of receptor serine/threonine kinases known as the type I and type II receptors [25]. The bound type II receptor complex phosphorylates and activates the type I receptors that then propagate the signal by phosphorylating intracellular Smad2 and Smad3. Other forms of inhibitory Smads can also negatively control the TGF-β pathway activity in response to antagonistic feedback [24]. The opposing actions of TGF-β receptor kinases and Smad phosphatases keep Smad proteins in a rapid phosphorylation-dephosphorylation cycle, tying signal flow to receptor activity. Activated Smad complexes additionally recruit transcriptional coactivators, corepressors, and chromatin remodeling factors. Through this combinatorial interaction with different transcription factors, a common TGF-β stimulus can activate or repress hundreds of target genes. The signaling model we use here (shown in Fig. 2) retains the essential characteristics of the pathways even though it is greatly simplified to facilitate analysis.

For intracellular reactions, the model is based on the following steps: (i) extracellular TGF-β (T) is first bound to available free receptors (R) on the cell surface where both type I and type II receptors have been merged. (ii) TGF-β bound receptors (TR) phosphorylate Smad2/3, represented as a single Smad entity (S). (iii) Since it was shown the complex are internalized through two distinct endocytic routes, the clathrin-dependent endocytosis and the caveolar lipid-raft mediated endocytosis [9,26], the internalization and subsequent degradation of TGF-Receptor complex is included in the model. (iv) The receptor concentration is generally stable after the initial transient stage. So, the equivalent amount of receptor degraded with TGF inside the cell is regenerated. (v) The reversing effect of phosphatase is represented by the dephosphorylation of the phosphorylated Smad complex (S_P). (vi) Production of TGF-β is modeled using a pSmad mediated Hill function with subsequent intracellular to extracellular secretion. The symbols for the species involved and their definitions are given in Table 1. The reactions involved in the model starts with the TGF ligand binding along the surface, and subsequent binding with intracellular Smad proteins.

$$T + R \rightleftharpoons TR$$

$$TR + S \rightleftharpoons TRS$$

The TGF-receptor-Smad (TRS) complex produces phosphorylated Smad following a Michaelis–Menten kinetics. However, pSmad also gets dephosphorylated inside the cell.

$$TRS \longrightarrow TR + S_P$$

$$S_P \longrightarrow S$$

Table 3
Set of ordinary differential equations governing intracellular reactions.

$$\frac{dR}{dt} = k_1^- TR - k_1^+ T \cdot R + k_d TR \tag{2.4}$$

$$\frac{dTR}{dt} = k_1^+ T \cdot R - k_1^- TR + k_T^- TRS - k_T^+ TR \cdot S + k_T^0 TRS - k_d TR \tag{2.5}$$

$$\frac{dTRS}{dt} = k_T^+ TR \cdot S - k_T^- TRS - k_T^0 TRS \tag{2.6}$$

$$\frac{dS}{dt} = k_T^- TRS - k_T^+ TR \cdot S + k_S S_P \tag{2.7}$$

$$\frac{dS_P}{dt} = k_T^0 TRS - k_S S_P \tag{2.8}$$

$$\frac{dT^{in}}{dt} = \frac{r_1 S_P^n}{r_2^n + S_P^n} - k_3 T^{in} \tag{2.9}$$

Production of TGF-β inside the cell with the aid of phosphorylated Smad follows a Hill function kinetics which will be discussed in detail in Section 4. The secretion of TGF-β is considered proportional to its concentration inside.

In constructing these ODE system, most of the relevant reaction constants and parameters were chosen from the ones reported in literature [30,18,4]. In some cases, reported parameters vary by the source and some are reported with a range of values depending on cell line. Additionally, model features such as TGF-receptor degradation after endocytosis and TGF secretion rate may have unknown rate parameters. In those cases, parameters (reported in Table 2) have been adjusted to match the representative cases to available experimental data. The system of ODEs is shown in Table 3.

3. Numerical methods

In our present work, the mixed set of governing equations involving ODEs for intracellular and a PDE for extracellular dynamics are solved at each time step. We use an immersed interface method (IIM) with fast algorithm [21] to solve Eqs. (2.1)–(2.3) for calculating TGF-β concentrations with second order accuracy. Time dependence in Eq. (2.1) arises from the time dependence of the concentrations of T, R, TR and T^{in}. At each time step we set the jump in flux $v(s) = S$ where,

$$S = k_1^- TR - k_1^+ T \cdot R + k_3 T^{in}$$

and the jump $w(s) = w(s)_{old} + G$, where

$$G = \Delta t \cdot S \cdot \varepsilon$$

Here, Δt is the time-step, and ε is the ratio of cell perimeter to cell area. G is the net change in TGF-β concentration during the time step assuming that the net TGF-β released at the surface is uniformly distributed throughout the domain. Details of the immersed interface (IIM) algorithm used for the solution can be found in [13,22]. The intracellular reaction kinetics are captured by solving the system of ordinary differential equations over each time step using a fourth order Runge–Kutta (RK) method. In principle, the dynamics of TGF-β in the extracellular domain is governed by a time dependent partial differential equation. In this preliminary study, we employ a quasi-steady state approximation for TGF dynamics. The dynamics of TGF-β is governed by a time and spatially dependent reaction diffusion equation (Eq. (2.1)). The source terms on the right side of Eq. (2.1) includes delta function terms on the immersed membrane boundary. These terms originate from the cell surface chemical reactions for the binding-unbinding of TGF-β with cell surface receptors, as well as secretion of TGF produced inside. The cell surface reactions are coupled to the TGF-SMAD intracellular reactions which are presented as a system of ODE and solved over time. This results in a time and space dependent source term and jump conditions for Eqs. (2.1)–(2.3). At each time step, we solve Eq. (2.1) with updated source terms and jump conditions derived from the time dependent ODE solutions. Away from the singular cell boundary, the time rate of change of TGF-β is governed by the small TGF-β degradation rate (1/(250 min)). Thus dT/dt would be small away from the boundary.

In this study, the interface is not moving although it is not a requirement for the numerical method used. In the solution procedure, the jumps were calculated at each time step from the previous solution at the control points on the cell membrane boundary. Cubic splines are used to define the cell interface passing through the control points (x_k, y_k), where $k = 1, \ldots, 128$, with equal spacing. The cells considered in these simulations have a diameter of 10 μm and the time-step for the global solution was 0.01 seconds. We use a uniform (512×512) Cartesian grid with equal mesh size for the 100 μm square domain. Fig. 3 illustrates the overall solution algorithm used in this study for both extracellular and intracellular regions.

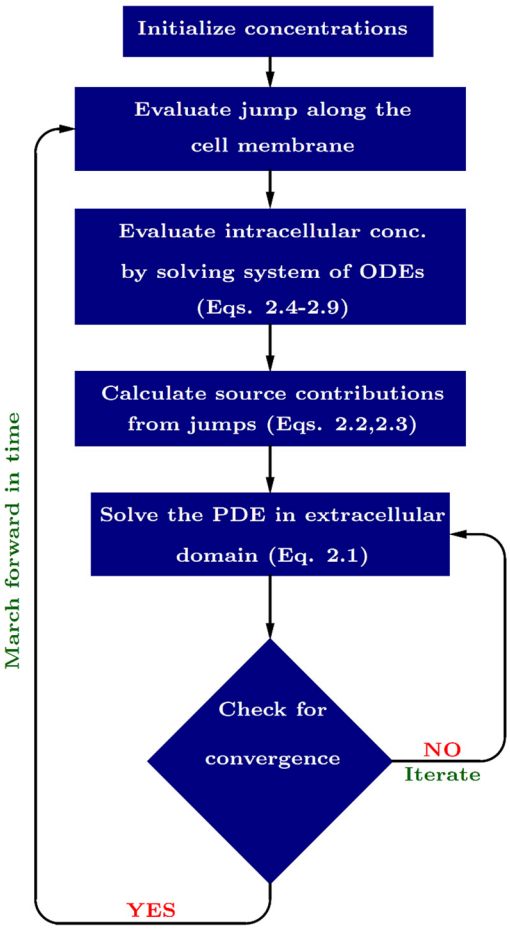

Fig. 3. Flowchart for the hybrid algorithm designed to solve the coupled temporal intracellular and the spatiotemporal extracellular domain. Since the extracellular concentration changes due to cellular consumption and secretion, it is necessary to evaluate extracellular TGF levels at each time-step. This also directly affects the intracellular production thus creating a coupled system that is solved by iterations.

4. Numerical results

The cellular response to TGF-β depends on the number of bioactive TGF molecules, and also the duration of the exposure [38]. The response however, is also dependent on the receptor concentration, receptor internalization and recycling dynamics, as well as presence of others cofactors such as BMP, MMP etc. [36]. From the modeling perspective, this varied level of dependence introduces a large number of unknowns in terms of reaction parameters and their dynamics. In our model we use parameter values used by Kim and Othmer [18]. We also use some parameters from the studies reported by Zi et al. such as the surface receptor and Smad concentrations [38].

In Fig. 4 and 5, we show a comparison of model simulation results with experimental results from Clarke et al. [6]. The cell lines used in the experiments were PE25 mink lung epithelial cells. However, the parameters used by Kim and Othmer were based on HaCaT cell lines as reported by Schmierer et al. [30] and Hendriks et al. [12]. The *in vitro* studies in [6] were initiated with a uniform dose of extracellular TGF-β added to the cells in the cell culture. Measurements of TGF-β and pSmad levels were taken at 9 time points over a 24-hour period. The gradual depletion of TGF in the cell culture has three primary contributing factors. These include the reversible binding of TGF-β reaction with cell surface receptors, endocytosis and degradation of receptor bound TGF-β and the extracellular basal degradation. Depending on the extracellular concentration and the concentration of surface receptors, the TGF-receptor association-dissociation reaction starts immediately Although the lower TGF-β concentrations of 10 and 25 pM are predicted reasonably well by the model (Fig. 4(a) and 4(b)), with no TGF-β production the model consistently under-predicted TGF-β levels for the 200 pM case (Fig. 4(c) and Fig. 5(b)). Kojima et al. working with human breast carcinoma MCF-7-ras cells and fibroblasts proposed an autocrine signaling mechanism with pSmad dependent TGF production. Since pSmad is directly linked to downstream nuclear transcriptional activity, we introduced a pSmad mediated TGF-β upregulation. In the model the production is represented by a Hill function which allows TGF-β production at higher pSmad levels. The Hill function represents a number of intracellular processes involving reaction and binding of different Smad proteins, nuclear shuttling and transcriptional activation. In almost all cases these

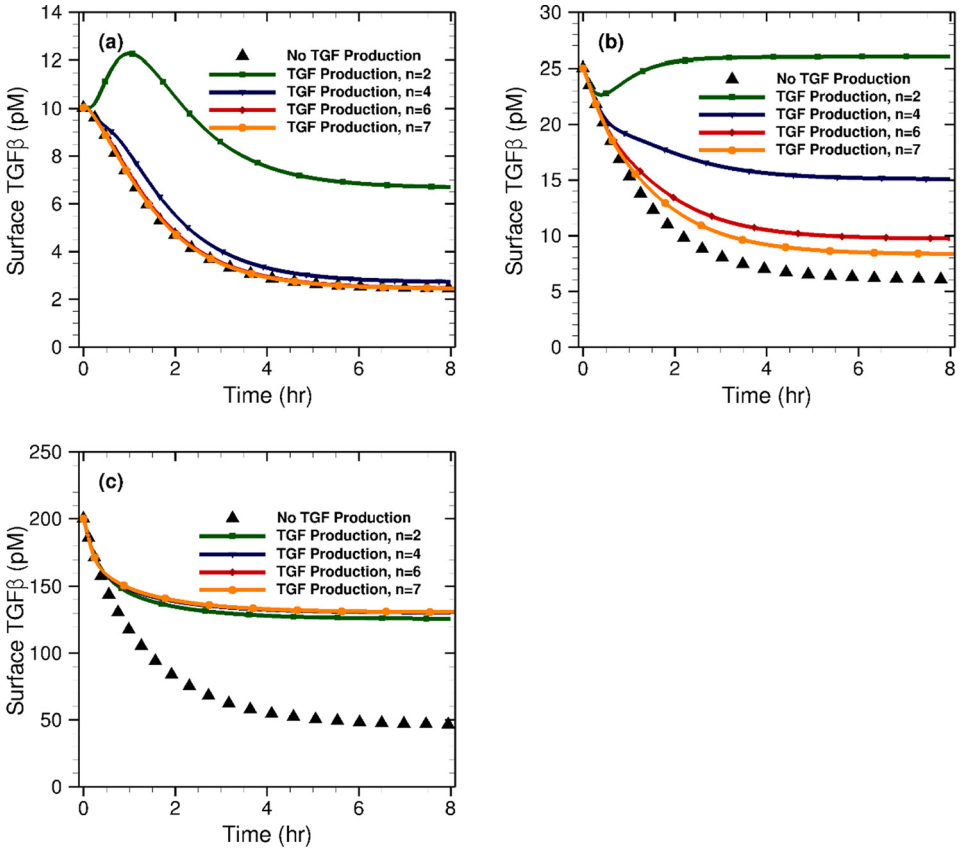

Fig. 4. TGF-β dynamics depending on cellular activity. A pSmad dependent Hill function of order 'n' is used to model intracellular TGF-β production. Secretion of produced TGF-β to the ECM slows down the rate of drop in bulk TGF. The kinetics of TGF-β decay is related primarily to available receptor concentrations and the rate of TGF-receptor complex internalization. Subfigures (a), (b) and (c) represent temporal extracellular evolution of TGF-β for initial concentrations 10, 25 and 200 pM respectively.

reaction parameters are unknown. Therefore, the use of generalized TGF-β production term streamlines the model without sacrificing crucial detail. Different orders for the Hill function (n in Eq. (2.9)) were tested and several cases are also included in Fig. 4.

After the adjustment, the model with $n = 7.0$ was chosen for the goodness of fit as shown in Fig. 5(a) while the exact same cases are presented in Fig. 5(b) without TGF production. It should be noted that, aside from the initial TGF-β condition, all parameters in the three cases (10, 25, 200 pM) are identical. Comparing Fig. 5(a) and 5(b), it is evident the autocrine TGF production behavior used in our model successfully captures the experimental TGF evolution. At the same time, it corroborates the autocrine signaling hypothesis suggested by Kojima et al. [20] developed different cell lines and experimental conditions. Although a number of previous studies have explored the TGF-Smad dynamics [38,30,18], they do not include endogenous cellular production of TGF necessary for autocrine TGF signaling. Further validation of the numerical method along with detailed convergence tests and maximum error percentages have been presented in our previous publication [13].

The model pSmad predictions succeed in portraying the steady state behavior for the higher range of extracellular TGF (Fig. 6(c)). For the lower end (10 and 25 pM), although the initial transient is captured by the model, the experimental data shows a decay in pSmad activity in the long term which is not captured by our model. One reason for this could be lack of any basal degradation for Smad and pSmad in the model. Since the experimental data was calculated on a pSmad per cell basis, we represent the comparison in normalized form showing the qualitative match in pSmad temporal behavior. Kim and Othmer also presented evolution of pSmad for different levels of TGF (Fig. 5(H) in [18]), but they have kept the TGF concentrations fixed through the simulation in the ODE model. Nevertheless, their results for both low (1pM TGF, black line) and high level (400 pM TGF, red line) show comparable pSmad trends as ours. Although the pSmad numerical results show good agreement with the experimental results, stronger agreement could be obtained by adjusting the pSmad phosphorylation-dephosphorylation rates based on TGF-β availability as suggested in [37]. Additionally, the Smad pathway could be made more realistic by introducing more detailed Smad dynamics including Smad2 and Smad4 binding as well as cytoplasmic to nuclear shuttling.

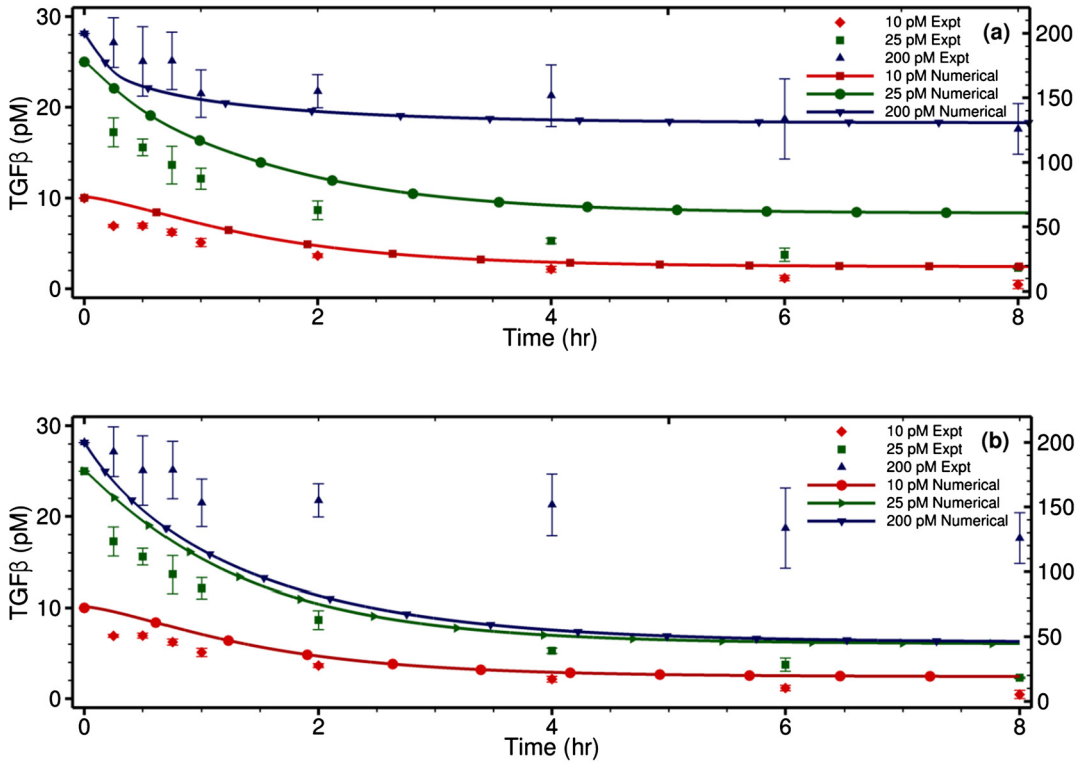

Fig. 5. Comparison with experimental data for TGF-β activity (a) with intracellular production and (b) without intracellular production for different initial concentrations with experimental data from [6]. Except initial concentrations, all parameters are the same as reported in Table 2.

In a tumor microenvironment, different types of cells behave differently upon TGF-β signaling [17]. In Fig. 7, we show behavior of two different cell types where one has the same parameters as chosen for model validation, and the second type includes a constant rate of TGF-β production. With initial external TGF-β levels set at 80 pM, we see an initial rise of intracellular TGF-β in both cases. However, the high rate of production and secretion from the second cell (Fig. 7(b)) results in a continuous build-up of extracellular TGF-β. In contrast, the intracellular TGF-β levels reach a steady state after the initial rise showing an overall balance in production, secretion and degradation. Although the extracellular measurements for TGF-β have been done in several experimental studies, it would be interesting to see additional intracellular measurements which would lead to a more complete understanding of intracellular reactions. The overall TGF-β levels across the domain are shown for the two cases in Fig. 8. Here, the distribution of TGF-β in the domain is affected by the location of the cell and whether it is producing or consuming as shown in Fig. 8(b) and 8(d). While contours of the domain are shown at a given instant (after 30 min), the cuts across the cell (Fig. 8(a) and 8(c)) show the evolution of TGF-β across the domain over 4 h. We note that the spatial variations are quite small in the field plots for the cases presented. Significant spatial variations are observed in our model with larger imposed flux jump conditions at the cell boundary. Using the parameters values based on values reported in the literature, the jumps were not strong enough to create a significant spatial variation in the field plots.

Finally, we investigate a two-cell case with both cells having the same reaction parameters and production/secretion characteristics (Fig. 9). Although the bulk extracellular TGF-β level remains largely unaffected, the field plots show the deterministic effect of cell location in the domain in determining the distribution after 30 min. Variation in the TGF-β distribution in the spatial domain is a direct function of the TGF-β diffusivity, as well as the source/sink contributions arising from secretion or absorption of TGF-β along the cell surface. This effect can be more accentuated in cases where two completely different types of cells are placed together. As the concentration field in Fig. 9(b) suggests, the location of cells in the microenvironment can determine which regions of the domain remains rich in TGF-β. In a growing cancer environment, this has implications in directing the direction of tissue growth and the progression of invasive phenotypes. In future works, we will explore conditions with cellular parameters for two different cell types that will also allow us to investigate paracrine as well as autocrine signaling in our TGF-β/Smad model.

5. Conclusions

The TGF-β pathway contributes significantly to a broad spectrum of tumor–stroma interactions in both pre-cancerous and malignant stages, creating a favorable microenvironment for tumor initiation, cancer cell growth and metastasis, and

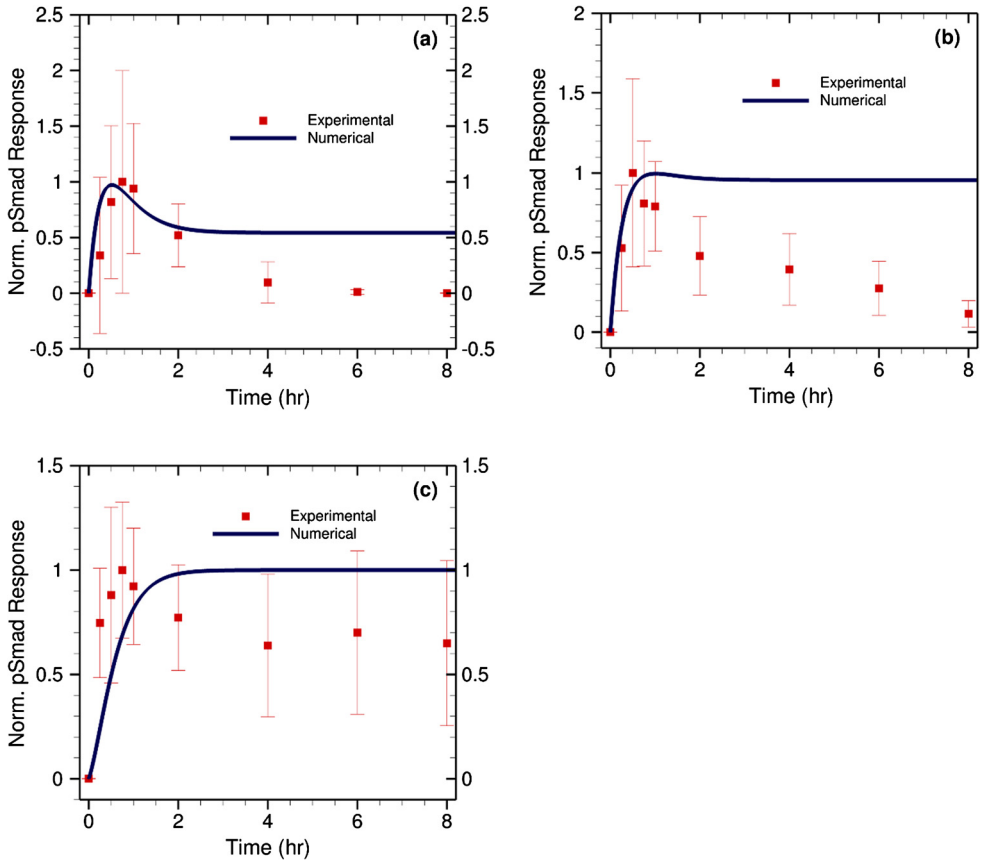

Fig. 6. The pSmad response for (a) 10 pM, (b) 25 pM and (c) 200 pM of initial extracellular TGF dosage. Each case has been normalized with respect to the maximum response level for that case. Data from experimental response by Clarke et al. [6] are included for validation.

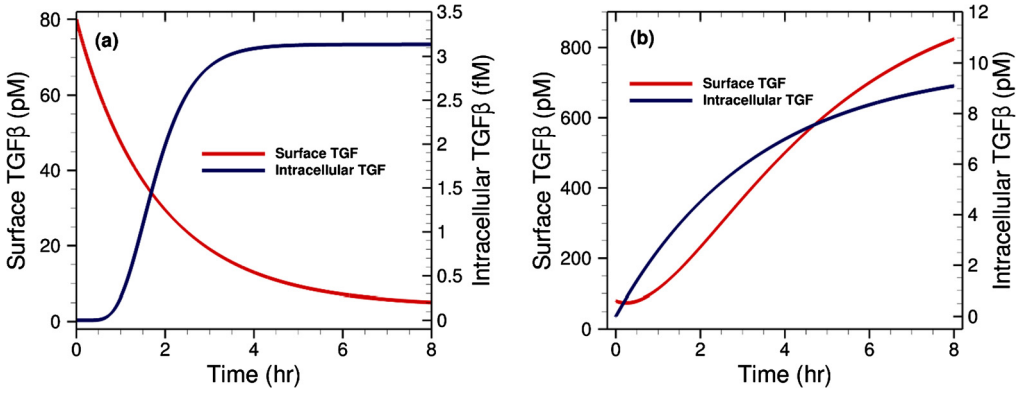

Fig. 7. Surface and intracellular levels of TGF-β for two different types of cell. (a) The cell has the same parameters as in validation simulations (Fig. 5), (b) Cell with same parameters as (a) with additional constant TGF production of 0.01 nM/min. For both cases, initial extracellular TGF level was set at 80 pM.

establishing a key thread of pro-tumoral activities throughout the steps of carcinogenesis. The effects on the microenvironment establishes interdependencies between the cancer cells that display altered or no response to TGF-β, and the TGF-β-stimulated and responsive stromal cells. Thus, TGF-β targeted therapy may affect cancer cells by indirect, microenvironment-mediated, mechanisms throughout all the steps of carcinogenesis.

In this preliminary study of the TGF-β/Smad signaling pathway, we developed a simplified model and showed that the model could produce qualitatively similar results to a set of experiments over a 24-hour time course. We showed that TGF-β production as hypothesized by Kojima et al. [20] may be required in order to match all the dosage results. We applied the

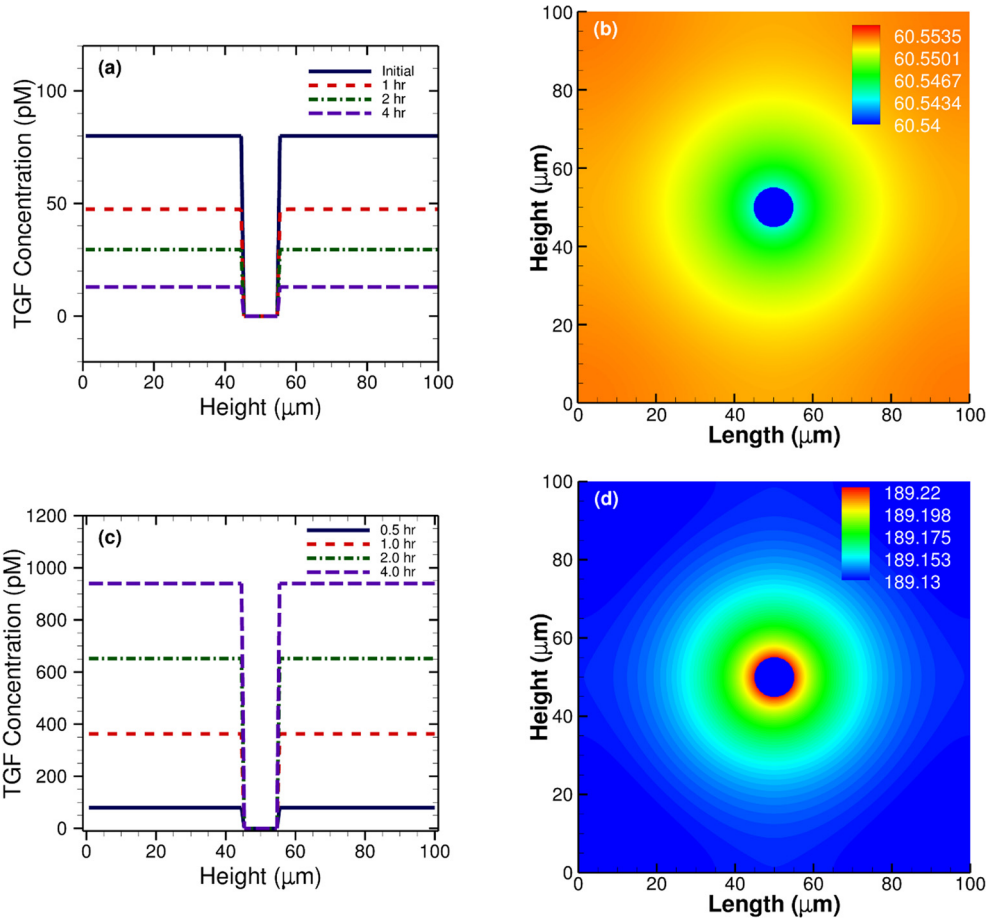

Fig. 8. Variation of domain TGF distribution over time for two different kinds of cells. Model details are the same as in Fig. 7. (a) Decline of TGF level from initial 80 pM in the domain over 4 h and (b) corresponding field at 30 min. (c) Rise of domain TGF over 4 h due to cellular production and secretion and (d) corresponding field at 30 min.

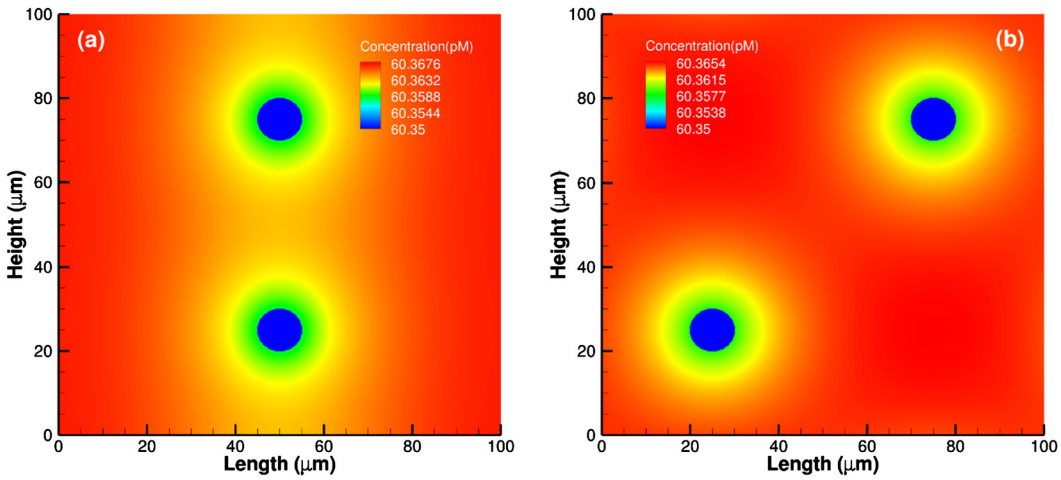

Fig. 9. Variation in TGF distribution in the extracellular domain with periodic boundaries. For both cases initial TGF concentration is 80 pM in the domain and the parameters are the same as reported in Table 2. (a) Cells are in vertical orientation with separation distance of 50 μm. (b) Cells are in diagonal configuration with a separation distance of 70.71 μm.

model to two different cell types showing significant variation from similar initial conditions, and discussed their possible implications in the tumor microenvironment.

Numerical models coupling the intracellular signaling network with extracellular signals and nutrients and effects of neighboring cells can answer a number of other critical questions such as, when does TGF-β act as a metastatic signal and how does the distance and number of carcinoma associated fibroblasts affect the pathway. More importantly, on the tissue level, this type of model can provide valuable knowledge to be used to study therapeutic effectiveness of different drugs. Our approach to the tumor microenvironment as a collection spatial and temporally active dynamic processes can be extended in future to investigate the intercellular cross-talk and their effects on tumor progression

Acknowledgements

This work was supported in part by the National Science Foundation under Grant No. DMS-1317671.

References

[1] M.B. Albro, R.J. Nims, A.D. Cigan, K.J. Yeroushalmi, T. Alliston, C.T. Hung, G.A. Ateshian, Accumulation of exogenous activated TGF-β in the superficial zone of articular cartilage, Biophys. J. 104 (8) (2013) 1794–1804.
[2] F.R. Balkwill, M. Capasso, T. Hagemann, The tumor microenvironment at a glance, J. Cell Sci. 125 (23) (2012) 5591–5596.
[3] D.A. Beacham, E. Cukierman, Stromagenesis: the changing face of fibroblastic microenvironments during tumor progression, Semin. Cancer Biol. 15 (5) (2005) 329–341.
[4] S.-W. Chung, F.L. Miles, R.A. Sikes, C.R. Cooper, M.C. Farach-Carson, B.A. Ogunnaike, Quantitative modeling and analysis of the transforming growth factor beta signaling pathway, Biophys. J. 96 (5) (2009) 1733–1750.
[5] D.C. Clarke, M.D. Betterton, X. Liu, Systems theory of Smad signalling, Syst. Biol. 153 (6) (2006) 412–424.
[6] D.C. Clarke, M.L. Brown, R.A. Erickson, Y. Shi, X. Liu, Transforming growth factor beta depletion is the primary determinant of Smad signaling kinetics, Mol. Cell. Biol. 29 (9) (2009) 2443–2455.
[7] D.C. Clarke, X.D. Liu, Decoding the quantitative nature of TGF-beta/Smad signaling, Trends Cell Biol. 18 (9) (2008) 430–442.
[8] G. De Crescenzo, P.L. Pham, Y. Durocher, M.D. O'Connor-McCourt, Transforming growth factor-beta (TGF-β) binding to the extracellular domain of the type II TGF-β receptor: receptor capture on a biosensor surface using a new coiled-coil capture system demonstrates that avidity contributes significantly to high affinity binding, J. Mol. Biol. 328 (5) (2003) 1173–1183.
[9] G.M. Di Guglielmo, C. Le Roy, A.F. Goodfellow, J.L. Wrana, Distinct endocytic pathways regulate TGF-β receptor signalling and turnover, Nat. Cell Biol. 5 (5) (2003) 410–421.
[10] Y. Drabsch, P. ten Dijke, TGF-beta signalling and its role in cancer progression and metastasis, Cancer Metastasis Rev. 31 (3–4) (2012) 553–568.
[11] C.H. Heldin, K. Miyazono, P. tenDijke, TGF-beta signalling from cell membrane to nucleus through SMAD proteins, Nature 390 (6659) (1997) 465–471.
[12] B.S. Hendriks, G. Orr, A. Wells, H.S. Wiley, D.A. Lauffenburger, Parsing ERK activation reveals quantitatively equivalent contributions from epidermal growth factor receptor and HER2 in human mammary epithelial cells, J. Biol. Chem. 280 (7) (2005) 6157–6169.
[13] M.R. Hossan, R. Dillon, P. Dutta, Hybrid immersed interface-immersed boundary methods for AC dielectrophoresis, J. Comput. Phys. 270 (2014) 640–659.
[14] G.J. Inman, Switching TGF beta from a tumor suppressor to a tumor promoter, Curr. Opin. Genet. Dev. 21 (1) (2011) 93–99.
[15] G.J. Inman, F.J. Nicolas, C.S. Hill, Nucleocytoplasmic shuttling of Smads 2, 3, and 4 permits sensing of TGF-beta receptor activity, Mol. Cell 10 (2) (2002) 283–294.
[16] S.B. Jakowlew, Transforming growth factor-beta in cancer and metastasis, Cancer Metastasis Rev. 25 (3) (2006) 435–457.
[17] R. Kalluri, M. Zeisberg, Fibroblasts in cancer, Nat. Rev. Cancer 6 (5) (2006) 392–401.
[18] Y. Kim, H.G. Othmer, A hybrid model of tumor–stromal interactions in breast cancer, Bull. Math. Biol. 75 (8) (2013) 1304–1350.
[19] Y. Kim, M.A. Stolarska, H.G. Othmer, The role of the microenvironment in tumor growth and invasion, Prog. Biophys. Mol. Biol. 106 (2) (2011) 353–379.
[20] Y. Kojima, A. Acar, E.N. Eaton, K.T. Mellody, C. Scheel, I. Ben-Porath, T.T. Onder, Z.C. Wang, A.L. Richardson, R.A. Weinberg, A. Orimo, Autocrine TGF-beta and stromal cell-derived factor-1 (SDF-1) signaling drives the evolution of tumor-promoting mammary stromal myofibroblasts, Proc. Natl. Acad. Sci. USA 107 (46) (2010) 20009–20014.
[21] R.J. Leveque, Z.L. Li, The immersed interface method for elliptic equations with discontinuous coefficients and singular sources, SIAM J. Numer. Anal. 31 (4) (1994) 1019–1044.
[22] Z.L. Li, A fast iterative algorithm for elliptic interface problems, SIAM J. Numer. Anal. 35 (1) (1998) 230–254.
[23] J. Massague, How cells read TGF-beta signals, Nat. Rev. Mol. Cell Biol. 1 (3) (2000) 169–178.
[24] J. Massague, The TGF beta pathway in basic oncology, An. R. Acad. Nac. Farm. 71 (3) (2005) 525–534.
[25] J. Massague, TGF beta in cancer, Cell 134 (2) (2008) 215–230.
[26] H. Mitchell, A. Choudhury, R.E. Pagano, E.B. Leof, Ligand-dependent and -independent transforming growth factor-beta receptor recycling regulated by clathrin-mediated endocytosis and Rab11, Mol. Biol. Cell 15 (9) (2004) 4166–4178.
[27] F.J. Nicolas, K. De Bosscher, B. Schmierer, C.S. Hill, Analysis of Smad nucleocytoplasmic shuttling in living cells, J. Cell Sci. 117 (18) (2004) 4113–4125.
[28] G.I. Patterson, R.W. Padgett, TGF beta-related pathways – role of Caenorhabditis elegans development, Trends Genet. 16 (1) (2000) 27–33.
[29] D.R. Principe, J.A. Doll, J. Bauer, B. Jung, H.G. Munshi, L. Bartholin, B. Pasche, C. Lee, P.J. Grippo, TGF-beta: duality of function between tumor prevention and carcinogenesis, J. Natl. Cancer Inst. 106 (2) (2014).
[30] B. Schmierer, A.L. Tournier, P.A. Bates, C.S. Hill, Mathematical modeling identifies Smad nucleocytoplasmic shuttling as a dynamic signal-interpreting system, Proc. Natl. Acad. Sci. USA 105 (18) (2008) 6608–6613.
[31] K.E. Sung, N. Yang, C. Pehlke, P.J. Keely, K.W. Eliceiri, A. Friedl, D.J. Beebe, Transition to invasion in breast cancer: a microfluidic in vitro model enables examination of spatial and temporal effects, Integr. Biol. 3 (4) (2011) 439–450.
[32] P.T. Ten Dijke, M.J. Goumans, F. Itoh, S. Itoh, Regulation of cell proliferation by Smad proteins, J. Cell. Physiol. 191 (1) (2002) 1–16.
[33] M. Tian, J.R. Neil, W.P. Schiemann, Transforming growth factor-beta and the hallmarks of cancer, Cell. Signal. 23 (6) (2011) 951–962.
[34] J.M.G. Vilar, R. Jansen, C. Sander, Signal processing in the TGF-beta superfamily ligand-receptor network, PLoS Comput. Biol. 2 (1) (2006) 36–45.
[35] L.M. Wakefield, C.S. Hill, Beyond TGF beta: roles of other TGF beta superfamily members in cancer, Nat. Rev. Cancer 13 (5) (2013) 328–341.
[36] M. Zeisberg, J. Hanai, H. Sugimoto, T. Mammoto, D. Charytan, F. Strutz, R. Kalluri, BMP-7 counteracts TGF-beta 1-induced epithelial-to-mesenchymal transition and reverses chronic renal injury, Nat. Med. 9 (7) (2003) 964–968.
[37] Z.K. Zi, D.A. Chapnick, X.D. Liu, Dynamics of TGF-beta/Smad signaling, FEBS Lett. 586 (14) (2012) 1921–1928.
[38] Z.K. Zi, Z.P. Feng, D.A. Chapnick, M. Dahl, D.F. Deng, E. Klipp, A. Moustakas, X.D. Liu, Quantitative analysis of transient and sustained transforming growth factor-beta signaling dynamics, Mol. Syst. Biol. 7 (2011).
[39] Z. Zi, E. Klipp, Constraint-based modeling and kinetic analysis of the Smad dependent TGF-beta signaling pathway, PLoS ONE 2 (9) (2007).